Creation and identification of the two spin states of dicarbon antisite defects in 4*H*-SiC

J. W. Steeds, W. Sullivan, S. A. Furkert, and G. A. Evans
Department of Physics, University of Bristol, Tyndall Avenue, Bristol BS8 1TL, United Kingdom

P. J. Wellmann
Department of Materials Science and Engineering, University of Erlangen-Nürnberg, 91058 Erlangen, Germany
(Received 29 June 2007; revised manuscript received 8 February 2008; published 9 May 2008)

This paper deals with the positive identification by low-temperature photoluminescence microspectroscopy of the two spin states of the dicarbon antisites in 4*H*-SiC. The defects are created by high-dose electron irradiation at room temperature or by subsequent exposure to intense 325 nm radiation at temperatures up to 1300 °C. Identification was achieved by their formation and annealing characteristics, by the energies of their local vibrational modes, by the nature of their splitting in ^{13}C isotope enriched samples, and by comparison with published results of *ab initio* local density approximation calculations. Four related but different forms of this defect have been predicted, two with $S=0$ and two with $S=1$, and their calculated properties are consistent with the experimental results presented here. The excitation processes for the optical centers within the irradiated region are quite unusual. For a 488 nm laser excitation, both spin states of the defect are observed by up-conversion. For a 325 nm excitation, the optical centers are only observed at the periphery of the high-dose irradiated regions after the sample has been exposed to an intense 325 nm beam. In this case, the optical centers are mainly in the $S=0$ state. The centers are eliminated by annealing in the range of 800–950 °C.

DOI: 10.1103/PhysRevB.77.195203 PACS number(s): 61.72.J−, 61.80.Fe, 63.20.Pw, 81.05.Hd

I. INTRODUCTION

An understanding of the optical centers observed after electron irradiation damage of 4*H*-SiC is of considerable practical interest as described in the associated paper (Steeds and Sullivan[1]). The present paper concentrates on two aspects of a particular complex of lines at 463 nm in the low-temperature photoluminescence (PL) spectroscopy of electron-irradiated 4*H*-SiC that was originally reported Fig. 4 of Evans *et al.*[2] First, there is the question of the atomic origin of these lines. The low-temperature spectrum was briefly discussed in a subsequent publication reviewing the great variety of centers in electron-irradiated 4*H*-SiC and 6*H*-SiC . [3] The latter publication drew attention to some of the features of the triplet that are explored in considerable detail here. A connection was also suggested between this triplet in 4*H*-SiC and the P-T lines (not labeled at that time) in 6*H*-SiC. A more detailed analysis of five optical centers in 6*H*-SiC, labeled the P-T centers, which were interpreted as involving C-C dumbbells, was then published.[4] Although this paper suggested that the optical centers responsible for the PL were split carbon interstitials, subsequent theoretical work investigated this proposal in more detail. One group (Gali *et al.*[5]) arrived at the conclusion that the P-T centers were, in fact, created by dicarbon antisite defects, the other group (Mattausch *et al.*[6]) weighed up the arguments in favor of the dicarbon antisite compared with the split carbon interstitial. In the present work, we shall present evidence that the 463 nm complex in 4*H*-SiC is, indeed, caused by dicarbon antisites in this material and show excellent agreement with the published results of calculations.

Second, there are fascinating and subtle issues related to the laser excitation of the centers and their creation, distribution, and annealing. These properties are important for investigating the possible presence of the defects in 4*H*-SiC and for understanding their possible relevance to device processing steps. The paper is organized to deal with these two aspects separately.

II. EXPERIMENTAL DETAILS

Most of the samples studied during the course of this investigation were irradiated at room temperature in a pure (ion-free), highly monochromatic, electron source of an especially modified transmission electron microscope (TEM) (Philips EM 430). The irradiations were performed locally on bulk specimens with an electron beam of circular cross section that had a diameter of either 100 or 200 μm and a uniform intensity distribution with a sharp cutoff at its perimeter. The electron energy was normally 300 keV, but lower-energy irradiations were also performed. For higher-energy irradiations, up to 1 MeV, high voltage TEMs at the Max Planck Institute in Stuttgart and at the Lawrence Berkeley Laboratory in California were made available.

After irradiation, the samples were studied by low-temperature PL microscopy using Renishaw micro-Raman systems fitted with Oxford Instruments cryogenic stages. One of these Renishaw systems was operated with a 325 nm He/Cd laser, the other used an argon-ion laser that was normally operated at 488 nm, but experiments were also performed with it by using 457.9 nm excitation. For the 325 nm operation, the laser spot size was approximately 5 μm in diameter with 3 mW of power at 100% operation (it was generally operated at 1% or 10%). For the 488 nm laser, the power level was <10 mW and was focused as a 3 μm spot. Three different modes of operation were commonly used and examples of each appear in the figures in this paper. These were the *spot mode*, with the laser incident at a chosen location on the sample; the *line-scan mode*, where spectra were collected at equally spaced points (typically 10 or 20 μm apart) along a chosen line; and the *mapping mode*, where the

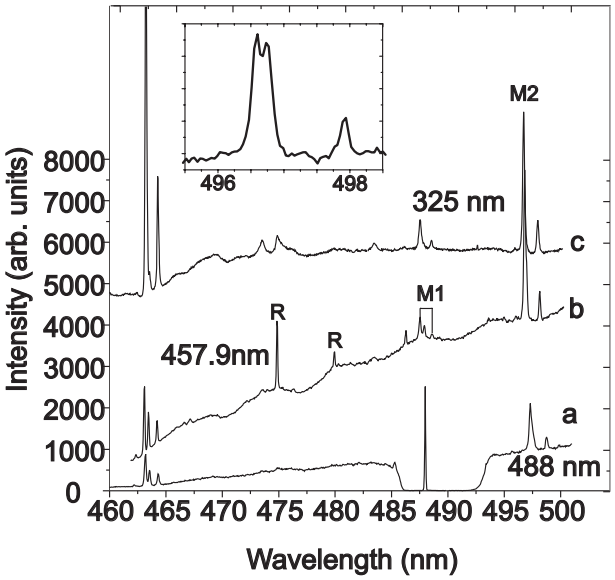

FIG. 1. Comparison of PL spectra of the 463 nm triplet obtained at different excitation wavelengths as follows: (a) 488 nm, (b) 457.9 nm, and (c) 325 nm. The dip in intensity near 488 nm in (a) is caused by the holographic notch filter used to attenuate the laser signal. Peaks *R* are caused by Raman scattering. The spectra were acquired at ~7 K. The inset shows splitting of the M2 LVM that is occasionally observed.

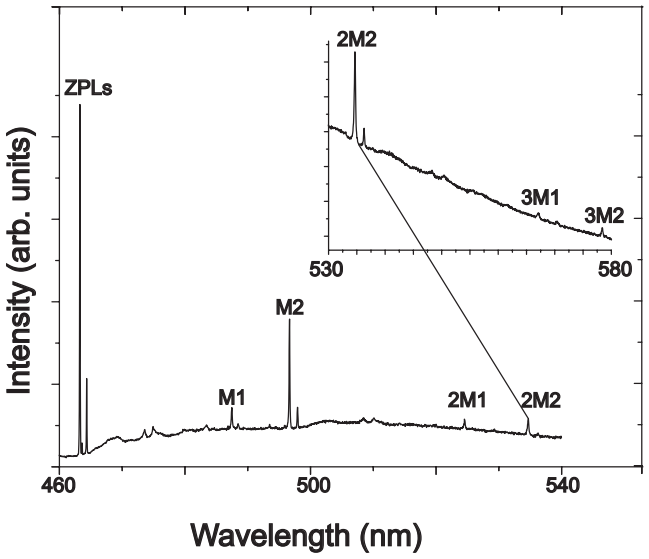

FIG. 2. Full spectrum of the 463 nm triplet using 325 nm excitation with the specimen at ~7 K. M1 and M2 are the lower- and higher-energy LVMs. *n*M1 and *n*M2 refer to *n*th order harmonics.

spectra were collected at a rectangular array of points.

The results presented here were obtained from a wide range of high quality epitaxial layers of 4*H*-SiC from different sources (more than 20). These included *n*-type material (N doped) with N concentration in the range of $5\times10^{13}-6\times10^{17}$ cm^{-3} and *p*-type (Al-doped) material (compensated and uncompensated) with Al concentration varying in the range of $5\times10^{15}-3\times10^{16}$ cm^{-3}. There was some variation of the overall intensity of the spectra from one sample to another, but no systematic trends were found. The irradiations were performed with electrons incident along [0001] on the silicon face of the samples mainly at energies from 250 to 300 keV to doses greater than 10^{19} e/cm^2. One sample was studied after irradiation by 300 keV electrons to a dose of 10^{18} e/cm^2. A few irradiations were performed at 5×10^{19} e/cm^2 on cleaved $\{10\bar{1}0\}$ faces of samples and these results were more variable.

More details of the experiments performed and the methodology employed are given in the associated paper (Steeds and Sullivan[1]), which concentrates on other centers that were found to have high-energy local vibrational modes after electron irradiation.

III. EXPERIMENTAL RESULTS AND ANALYSIS

A. Details relevant to the atomic configurations

A very common observation, made during the examination of TEM-irradiated 4*H*-SiC using 488 nm laser excitation [Fig. 1(a)], is the appearance of a triplet of lines at about 463 nm (463.2, 463.6, and 464.2 nm). A more complete spectrum of this triplet, undisturbed by the 488 nm notch filter, can be observed by using 325 nm excitation [Fig. 1(c)]. This triplet has a very strong coupling to local vibrational modes (LVMs) associated with it. With 325 nm excitation, these LVMs can be observed up to third order (Fig. 2). Both the 325- and 488-nm-excited spectra exhibit first-order high-energy LVMs (M2, Figs. 1 and 2), apparently in the form of a doublet at about 496 nm (496.5 and 497.8 nm, but see below for a clarification of this point). The 325 nm spectrum also reveals a lower-energy LVM doublet (M1, Fig. 2) at approximately 488 nm (487.3 and 488.4 nm), which is cut out of the 488-nm-excited spectrum by the notch filter.

As the 325 nm spectra are dominated by the first and third lines of the triplet and the 488 nm spectra depend on up-conversion and are disturbed by the notch filter, an attempt was made to investigate all three lines of the triplet spectrum by using the 457.9 nm line of the argon-ion laser. It was then clear that there are three components to the lower-energy LVM (M1) spectrum [Fig. 1(b)], not two as suggested by the 325 nm observations. Table I lists the observed LVM energies.

Lifetime measurements were carried out, using 457.9 nm laser excitation, on the emission (496.5 nm) associated with the higher-energy LVM but the decay time was shorter than the time resolution of the acousto-optic modulator used (10 ns). Some of the samples studied were irradiated with the electron beam overlapping a smooth cleavage edge. These were subsequently investigated edge on, so that the laser was incident on the cleaved edge itself, in order to perform polarization measurements on the triplet. These experiments were carried out at each of the three laser wavelengths employed but, as the results are mutually consistent, only the results of the 457.9 nm excitation will be used to illustrate the outcome because, in this case, each of the lines of the triplet is strong. For the electric field vector perpendicular to the *c* axis of the crystal, a triplet was observed, as in the case of incidence along [0001]. However, for the electric field vector parallel to [0001], the central line of the triplet be-

TABLE I. Wavelengths and energies of the three ZPLs of the 463 nm triplet together with the energies of their LVMs. The LVM data were obtained as a result of averaging data from several experiments carried out at different excitation wavelengths (see text for details) and have errors of 0.03 meV.

Optical center	(1) T1	(2) T2/T3	(3) T4
ZPL wavelength (nm)	463.15 ± 0.08	463.54 ± 0.08	464.26 ± 0.08
ZPL energy (eV)	2.676	2.674	2.670
First LVM energy (meV)	132.82 ± 0.03	132.53 ± 0.06	131.90 ± 0.05
Second LVM energy (meV)	179.86 ± 0.03	178.47 ± 0.06	180.03 ± 0.03

came stronger, sometimes very much stronger, than the other two (see Fig. 3), so that the outer two lines were sometimes hardly visible. The anisotropic (dipolar) emission from these polar centers plays an important role in these observations. The fact that the central line of the triplet is observed at all in the central region for the 488 nm radiation incident along [0001] is a consequence of its stronger emission, a situation that does not become apparent until the sample is viewed edge on. Not only does this establish that the outer lines are polarized mainly perpendicular to [0001], and the central line has a strong component polarized parallel to [0001], but it also provides a better understanding of the LVMs as will now be explained. First, as was indicated from a comparison of the previous 325 and 457.9 nm results, the central line of the lower-energy LVM triplet (M1) is associated with the central line of the zero phonon lines (ZPLs). Second, the measured wavelength of the high-energy LVM (M2) is slightly different for the two polarizations, which indicates that the shorter wavelength line of the earlier reported doublet is, in fact, a superposition of the LVMs of the lower-energy ZPLs of the triplet; the high-energy LVMs are, in fact, also a triplet. This conclusion is confirmed in the case of a sample annealed at 800 °C, where the width of the individual component lines of the triplet was sufficiently reduced to directly reveal the splitting of what had previously appeared to be a single line (see inset of Fig. 1). It has also been confirmed by using the second order of the diffraction grating to study the M2 spectrum. This procedure achieves enhanced spectral resolution (the energy difference is 0.8 ± 0.1 meV). The middle ZPL line of the triplet has its high-energy LVM at very slightly longer wavelength than that of the highest energy ZPL of the triplet. The final values for the energies of the LVMs are given in Table I. These values were obtained by averaging the wavelengths of peak fitted results for the six best 325 nm spectra, the four best 488 nm spectra, and the two best polarized 457.9 nm spectra (**E** parallel to [0001]).

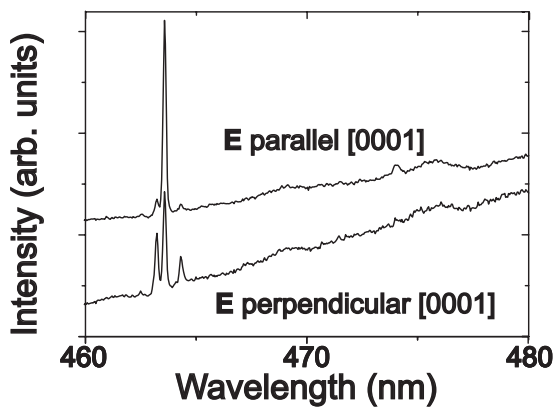

FIG. 3. Polarized 463 nm ZPL spectra from a chosen area of a sample mounted edge on to the incident 488 nm laser beam (on the {0110} face). Sample at ~7 K.

Another interesting result concerning this triplet was found by comparing the results of viewing the sample edge on, with the incident laser polarized either parallel or perpendicular to [0001]. The intensity of the central line of the triplet was considerably greater when the laser was polarized perpendicular to [0001] even though the emission at this wavelength was polarized parallel to [0001].

As a step toward the identification of the atomic nature of the defects responsible for the 463 nm triplet, a sample was prepared by sublimation growth with $30 \pm 5\%$ of ^{13}C replacing ^{12}C in 4*H*-SiC in the surface region. This sample was irradiated to 5×10^{19} e/cm^2 with 300 kV electrons and studied by low-temperature PL with 325 and 457.9 nm laser excitations. Under 457.9 nm laser excitation, the intensity of the middle line of the 463 nm triplet was somewhat reduced and appeared as a shoulder on the highest energy line (Fig. 4). A deconvolution of this spectrum (left inset of Fig. 4) gave values for the relative intensities of the three lines as shown in Table II. A longer exposure of the relevant part of the spectrum revealed a complex splitting in the spectral regions associated with the lower- and higher-energy LVMs (central and right insets of Fig. 4). With the sample mounted edge on to the incident 457.9 nm laser beam, polarized results were obtained for the ~463 nm spectrum (Fig. 5). Of particular interest is the spectrum for **E** parallel to [0001]. Here, the M2 spectrum exhibits threefold splitting, with three peaks in the approximate intensity ratios 1:4:4 (corresponding to 1/3 of the carbon atoms being the ^{13}C isotope. As only the middle ZPL of the triplet has this polarization, the threefold M2 splitting with these intensity ratios suggests the existence of close C-C dumbbells with 13/13, 12/13, and 12/12 pairs and a ^{13}C concentration of approximately 1/3. This is of the same order as the concentration deduced near the growth surface by secondary ion mass spectroscopy and Raman spectroscopy of this sample.[7] As a check on this conclusion, the ratios of the LVM energies were calculated, which yield the value of 1.04 for the ratio of the highest and lowest energies and 1.02 for the middle/lowest or highest/middle ratios. An attempt was therefore made to simulate the M2

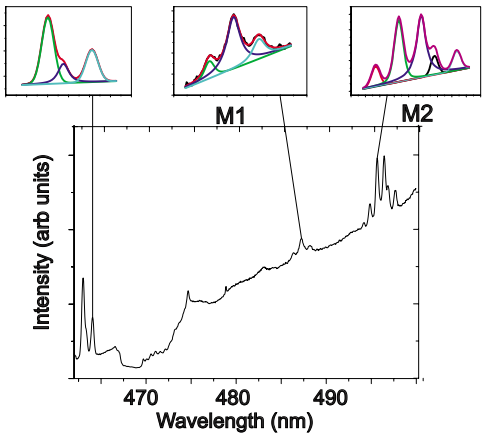

FIG. 4. (Color online) 457.9–nm-excited spectrum of the 463 nm triplet with the laser incident along [0001] on the Si surface of the ^{13}C-enriched sample at ~7 K. The insets show deconvolutions of the ZPLs (left), the lower-energy (M1) LVMs (mid), and the higher-energy (M2) LVMs (right).

spectrum shown in Fig. 4 by using the dumbbell model. A deconvolution of the triplet M2 spectrum (lower curve of Fig. 5) yielded a typical peak shape that was used in the simulation. It was assumed that each of the ZPLs in the deconvolved result (left inset of Fig. 4) contributed a threefold split M2 spectrum with 1:4:4 intensity ratios and that the relative contribution of each ZPL was governed by its relative intensity after deconvolution (see Table II). In order to determine the wavelengths of each of these contributions to the final M2 spectrum, the M2 LVM energies in Table I were each divided by 1.02 and 1.04, and the resulting energies subtracted from the relevant ZPL energy to yield the wavelengths shown in Table II. By adding together the nine separate contributions with the given weighting factors, the simulated form of the M2 spectrum shown in Fig. 6 was obtained. Figure 6(a) shows the contributions of the triplets from each of the individual ZPLs and Fig. 6(b) shows the comparison with experiment.

B. Excitation, creation, spatial distribution, and annealing

With the 488 nm excitation, the observation of the triplet was restricted to the irradiated area itself, and it often appeared quite strongly (by up-conversion) even though the

TABLE II. Data for the attempt to simulate the experimental results for the overlapping higher-energy LVMs of the ^{13}C-enriched sample. The relative intensities of the three ZPLs were obtained by a deconvolution of the data of Fig. 4 (left inset). The three lower columns give the calculated LVM peak positions for each of the three ZPLs.

High energy LVM	(1)	(2)	(3)
Relative intensity of ZPL	3.37	1	1.64
ZPL T1 (nm)	494.99	495.69	496.39
ZPL T2/T3 (nm)	495.07	495.77	496.46
ZPL T4 (nm)	496.18	496.87	497.58

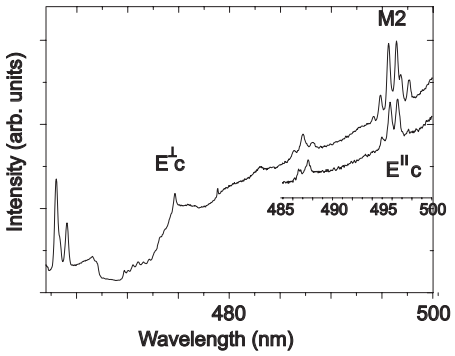

FIG. 5. 457.9-nm-excited polarized spectra of the 463 nm triplet with the laser incident on the ^{13}C-enriched sample edge on to the beam. The sample was at ~7 K.

emitted photons have considerably higher energy than the laser photons [Fig. 1(a)]. The up-conversion process, which is common to many optical centers in the irradiated 4*H*-SiC, will be discussed in Sec. IV C. The triplet intensity showed an approximately linear increase in intensity with increase in laser power and, in contrast, with the 325-nm-excited spectra, no hysteresis on returning to lower laser powers was observed. The intensity of the middle line of the three markedly varied, but the ratio of the intensities of the outer two lines varied less. For the outer two lines, the higher-energy line was always considerably stronger than the lower-energy line, usually at least twice as strong, but the middle line was sometimes stronger or weaker than the high-energy line. For

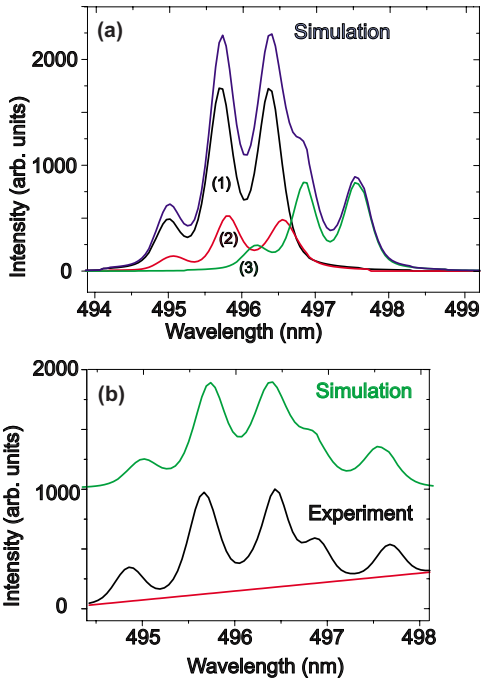

FIG. 6. (Color online) Results of an attempt to simulate the complex form of the M2 spectrum in Fig. 8. In (a), the envelope function is shown together with the three individual triplets (each with 1:4:4 intensity ratios) originating from each of the three ZPLs [indicated by (1), (2), and (3)]. (b) shows the result of simulation in comparison with the experimental result.

300 kV irradiations, under 488 nm laser excitation, there was no evidence of the 463 nm triplet for doses less than 10^{19} e/cm^2. For larger doses, the triplet intensity increased as the dose increased, with the two outer lines of the triplet growing more rapidly than the central line. Relatively few lower voltage irradiations have been investigated. At present, there is no evidence of the triplet, using 488 nm excitation of samples, after room temperature irradiation, at electron energies below 200 keV.

In the case of 457.9 nm excitation, the observed spectrum was limited to the irradiated region itself, and had a strong middle line, as with the 488 nm excitation. When 325 nm excitation was used, very different and, at first sight, quite puzzling characteristics of the PL were encountered [see Fig. 1(c)]. First, at low laser intensity (~0.03 mW into a 5 μm spot), none of the lines of the triplet was observed. Second, on increasing the laser intensity by 25 or 50 times, strong exposure-time dependent increase in intensity of the triplet emission was observed. As a result, the power dependence of the intensity is very dependent on acquisition time, time delay between acquisitions and spot position, and therefore sample drift. An investigation of the time dependence of the increase in the 463 nm intensities under constant 325 nm exposure showed an initial linear increase in intensity with a reduced rate at longer times, as illustrated in Fig. 7(a). A more graphic demonstration of this effect is shown in Fig. 7(b), where the initial absence of the triplet is changed to a very strong emission when high laser power is used. This increase was irreversible and was not eliminated by returning the sample to room temperature. This unusual behavior will be discussed in Sec. IV C. Third, in the case of 325 nm excitation, the middle line of the triplet was much weaker than the two outer lines, with the latter remaining in approximately the same intensity ratio as that observed by using a 488 nm excitation [compare Figs. 1(a) and 1(c)]. Fourth, this triplet was frequently limited to the peripheral region of the irradiated area, outside the region of irradiation itself (as illustrated in Fig. 7), although a few exceptions existed. In particular, after electron irradiation at 300 keV to a considerably lower dose (10^{18} $e\ \mathrm{cm}^{-2}$), the 463 nm triplet was only created within the irradiated area and not in the peripheral region. On reexamining the 325-nm-exposed samples, using 488 nm excitation, the original results were recovered, and there was no evidence of the triplet outside the irradiated area. After considerable exposure to high intensity 325 nm radiation, the intensity of the triplet sometimes became very strong, as strong as or stronger than that of the strongest of the so-called alphabet lines[8] [see Fig. 7(b)]. The changes introduced by the 325 nm exposure survived not only warming the sample to room temperature, but also annealing to quite high temperatures. Similar results were obtained on a sample irradiated to a dose of 10^{20} e/cm^2 at 150 keV. Quite different results were obtained from the sample irradiated to a dose of 10^{18} e/cm^2 at 300 keV. In this case, there was no triplet emission from the irradiated region with 488 nm excitation, but the intense 325 nm beam metastably induced it there; however, now not outside the irradiated area. The triplet spectrum induced in this way was similar to that obtained at the periphery of areas irradiated to higher electron doses.

Further experiments were devised to investigate the 325-nm-induced changes. Because the changes were local to

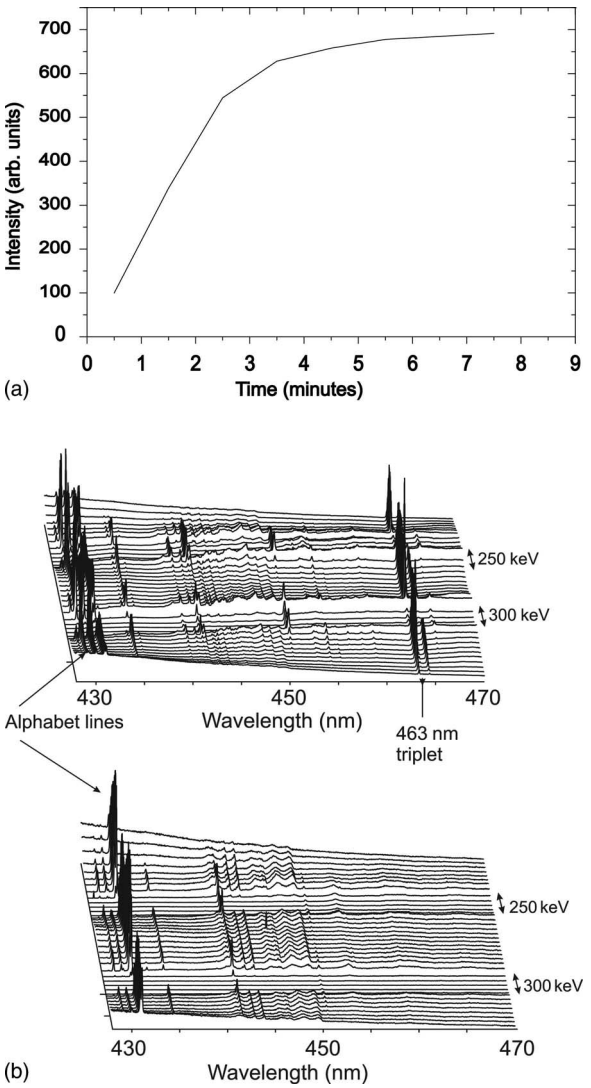

FIG. 7. (a) Increase in intensity of 463.2 nm emission with time of exposure to 325 nm beam at 10% power level; sample temperature ~7 K. (b) Comparison of line scans with 15 μm spacing across two electron-irradiated areas of a specimen (extending over the regions indicated by the double-headed arrows), one irradiated at 300 kV (lower) and the other at 250 kV (upper). The lower set of line scans was obtained first, using 1% of the power of the 325 nm laser (~0.03 mW into a 5 μm spot); the upper set was obtained later from the same region at 25% power. Note the appearance of the 463 nm triplet in the upper set of line scans and its absence from the lower set. Other more minor changes may also be observed and they are discussed in the associated paper (Ref. 1). The ZPLs in the wavelength range of 429–435 nm are the so-called alphabet lines. The spectra were acquired at ~7 K.

where the 325 nm beam had been concentrated, methods had to be devised that obtained data only from the exposed regions because of sample drift during prolonged experiments. Two techniques were found to be successful.[9] In the first technique, the high intensity laser was stepped across the peripheral region just outside the irradiated region with a dwell time of 3 min on a square array of points that are 40 μm apart. The exposed region was subsequently investigated at much lower laser power with a square array of

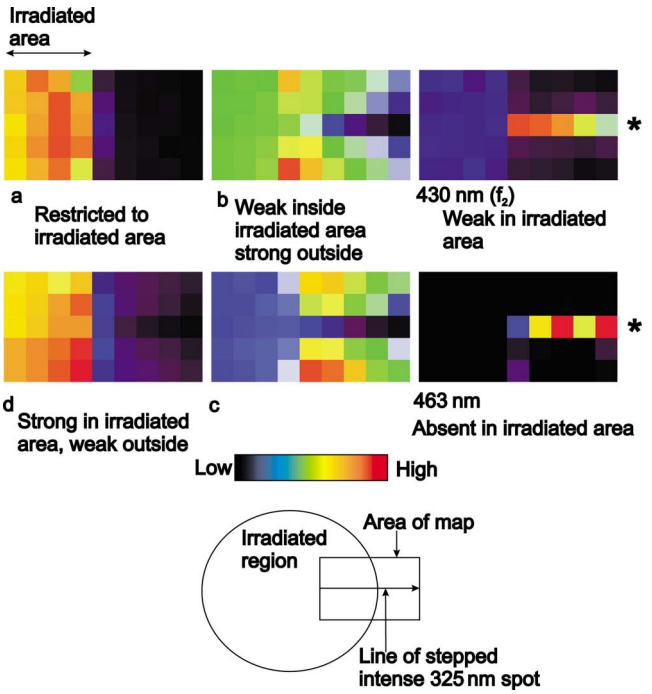

FIG. 8. (Color online) Integrated intensity maps of various optical centers obtained at 1% 325 nm laser power after exposure to an intense (%) 325 nm beam (5 min per point) stepped along a radial line (indicated by *) through the circular electron-irradiated area of 300 μm diameter and extending outside it. Maps labeled (a)–(d) are for the alphabet lines with this designation. The irradiated area (partially shown) is at the left side of each map (see diagram). The pixel size is 20×20 μm^2. The enhancements and diminutions survived annealing to 800 °C. The spectra were recorded at ~7 K.

points on a lattice of 5 or 7 μm. The local enhancements with 40 μm spacing were then clearly visible. However, the restriction of this enhancement to the periphery of the irradiated region made this technique more difficult to work with than an alternative. Here, a circular irradiated region was identified by the extent of the so-called alphabet line spectrum[7] at low laser power. A high intensity laser beam was then stepped outward from the center of this region along a radial line with steps of 5 μm spacing. Subsequent investigations at low laser power clearly revealed not only enhancement of 463 nm emission along this line but also colocated reduction in some of the alphabet lines. In particular, the alphabet line "*a*" was relatively unaffected; "*b*, *c*, and *d*" were reduced in intensity (see Fig. 8). In addition, a ZPL at 430 nm was also enhanced. The observed enhancements and diminutions survived several weeks at room temperature.

The temperature dependence of the triplet spectra was investigated by using both 325 and 488 nm excitations. The data for 325 nm excitation were obtained at low laser powers after a local enhancement by high power 325 nm exposure. This required keeping careful track of the locally enhanced region as the temperature of the sample was raised. On account of its low intensity, the data on the middle line of the triplet was relatively poor. For 488 nm excitation, although all three lines of the triplet could be measured, their relatively low intensities called for quite long exposure times (several minutes at the highest temperatures). A relatively small decrease in the intensities occurred in either case of excitation up to a temperature of 60 K. Above that temperature, for 325 nm excitation, the intensity of the highest energy ZPL of the triplet decreased more rapidly than the lowest energy line. Both had virtually disappeared by 125 K. The lower-energy LVMs at ~488 nm were too weak to be measured at 100 K, but the intensity of the higher-energy LVMs increased relative to the ZPLs over the range of 60–125 K. The high-energy line of the pair at ~496 nm more rapidly decreased with increase in temperature than the lower-energy line. Broadly similar results were obtained by using 488 nm excitation, but there were, in addition, data for the middle line of the triplet. Above 60 K, this middle line decreased in intensity significantly more slowly with increase in temperature than the two outer lines. As a result, the high-energy LVMs became increasingly dominated by the middle line. Above 100 K, this component of the triplet dominated the spectrum. A set of results is illustrated in Fig. 9.

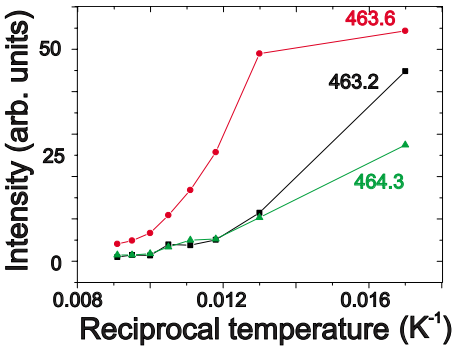

FIG. 9. (Color online) Temperature dependence of the ZPL integrated intensities as a function of reciprocal temperature.

The annealing behavior of the 463 nm triplet was quite complex and three different aspects have been investigated. These involved observations with 488 nm excitation, observations with 325 nm excitation, and observation after local enhancement using intense 325 nm excitation. The annealing experiments were performed under isochronal conditions in an ion-pumped vacuum or a nitrogen atmosphere for 30 min, mostly with 100 °C temperature intervals. For 488 nm excitation, the initial intensity of the middle line could be greater or less than that of the highest energy line of the triplet. At an annealing temperature of about 400 °C, the outer two lines increased somewhat in intensity, maintaining the same intensity ratio so that the intensities of the two higher energy lines became approximately equal. For anneals above 600 °C, all three lines of the triplet began to decrease in intensity, with the middle line more rapidly decreasing than the outer lines. Above a temperature of about 800 °C, somewhat depending on the sample, there was a rapid decrease so that the spectrum had virtually disappeared by 950 °C in all cases. The spatial location of the centers was unaffected by annealing, which always remains limited to the irradiated region itself. The loss of the spectrum after annealing at 950 °C could be the result of atomic changes to the centers or the elimination

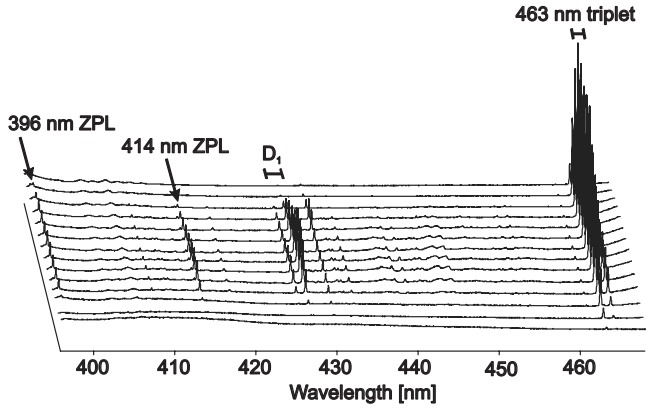

FIG. 10. Line scan across a 190 kV electron-irradiated region of a 4*H*-SiC sample annealed at 1300 °C, with the spectra being excited with 10% 325 nm laser power and the sample at ~7 K. This line scan shows the coexistence of the 463 nm triplet with other optical centers having LVMs [the ZPL at 414 nm is mentioned in the associated paper (Ref. 1)] and also with the well-known D_1 center. Note that in this example, the 463 nm PL extends across the center of the irradiated region with 325 nm excitation. The spacing of the points along the line was 15 μm.

of the up-conversion process. However, it should be noted that the up-conversion process still operated for other optical centers, including the DI center up to 1500 °C.

For the samples in which the triplet had been enhanced by prolonged low temperature, high intensity 325 nm exposure, subsequent experiments at higher temperature, using very low laser power, revealed that this enhancement was preserved up to annealing temperatures of 800 °C but was eliminated after annealing at 950 °C. For 1% power, 325 nm excitation of samples not previously exposed to higher laser powers, no evidence of the 463 nm triplet was detected. Using higher laser powers produced it at any temperature up to, and including, 1300 °C (when the alphabet lines had been eliminated) and it was generally restricted to the peripheral region, outside the irradiated area, with a few exceptions, as previously described. For samples annealed at 1100, 1200, and 1300 °C, the various alphabet lines were progressively eliminated[1] and the appearance of the triplet after high power 325 nm exposure could no longer be correlated with a decrease in their intensity. However, additional spectral lines appeared after these anneals[1] and two of these are of particular interest because they are found to be related to the dicarbon antisite pair and the tricarbon antisite.[1] Similarly, for samples irradiated with electron energies between 130 and 200 keV, and subsequently annealed at above 900 °C, no triplet emission was detected with 1% laser power, but its intensity strongly increased with higher laser powers, reaching a level that increased with an increase in accelerating voltage during irradiation so that, for example, for 150 keV, the triplet intensity was the most intense region of the spectrum (see Fig. 10 for the result at 190 keV). This increase apparently occurred without diminution of the intensity of any other optical center. The enhancement was found to be metastable, remaining on return to 1% power but vanishing after a further anneal at the original annealing temperature. The 463 nm triplet was not observed in any samples annealed at 1400 °C.

Experiments were performed on samples that had been irradiated at 1 MeV because MeV electron energies have been used frequently by others in past experiments involving electron irradiation. No significant differences were observed.

IV. DISCUSSION OF RESULTS

A. Atomic model

At the simplest level, the existence of optical centers having LVMs with energies of about 180 meV points to the presence of C interstitials. Additional important experimental results for arriving at an atomic model for the triplet of ZPLs discussed here are its thermal stability and the results obtained by isotopic substitution of 1/3 of the atoms on the carbon sublattice by ^{13}C. From the analysis of our experimental results in Sec. III, it is apparent that the highest energy local vibrational mode of each of the ZPLs is split into three components with the expected intensity ratios and vibrational energies of a C-C dumbbell in a sample containing 1/3 of its C atoms replaced by ^{13}C. Two simple atomic centers having this form are the C split interstitial on a carbon site and the dicarbon antisite. The former has been calculated as having low thermal stability, while the calculated thermal stability of the latter is consistent with its preservation to high temperatures. Moreover, our present results are rather similar to those reported for the five P-T centers in 6*H*-SiC and have similar ZPL energies when scaled to the band-gap energies of these polytypes. It is therefore appropriate to make a detailed comparison between our experimental results and the reported *ab initio* calculations.

B. Comparison with relevant calculations

Calculations have been performed by two groups using the local density approximation (LDA). Gali *et al.*[5] used a 96 atom supercell for their calculations for 4*H*-SiC with a harmonic approximation for the LVMs. Mattausch *et al.*[6] used 128 atom sites and what they call a defect molecule approximation. Where the results of these two groups overlap, they agree quite closely. In particular, both calculated local vibrational mode energies and they agree that the most accurate values are obtained for the most strongly bound modes. Gali *et al.*[5] quoted an accuracy of 5 meV for these modes, Mattausch *et al.*[6] quoted 10 meV as the maximum value of uncertainty. Their calculated energies are shown in Table III. Both agree that there is a low-spin ($S=0$) state and a slightly lower-energy high-spin state ($S=1$), both with C_{1h} symmetry. Additional splittings caused by spin-orbit coupling or different m_s values have not yet been calculated and are not likely to be resolved in the experiments discussed here. Each of these states is associated with a pseudohexagonal or pseudocubic location of the dicarbon antisite, which leads to a total of four defects labeled T1–T4 here. Mattausch *et al.*[6] calculated the dissociation energies for the two sites as 3.6 eV $(C_2)_{Si,h}$ and 3.5 eV $(C_2)_{Si,k}$ and concluded that the defect will be neutral for a Fermi level $\mu_F 1.27 < \mu_F < 2.04$ eV for 4*H*-SiC. Gali *et al.*[5] argued that in the neutral charge state, the centers are isoelectronic in nature, but if this is true, then

TABLE III. The calculated LVM energies in meV for the dicarbon antisite defect (taken from Ref. 6). ls=low spin; hs =high spin.

k		*h*	
ls	hs	hs	ls
102.3	101.5	100.2	103.0
119.7	120.7	121.0	121.9
135.0	136.2	136.4	136.2
139.1	137.6	137.6	139.3
178.0	177.0	177.1	179.4

longer lifetimes would be anticipated than those recorded here.

Not all of the LVMs shown in Table III are likely to be detected by PL experiments. The highest energy mode is a stretching mode and should be detected. Of the two lower-energy modes at around 138 meV, one is approximately symmetric and should be observed; the other is approximately antisymmetric and should be undetected. With this information, it is possible to make a detailed comparison with the experimental results (Table IV). The high-energy LVMs (M2) of the two high-spin states are so close in energy that they would not be resolved in our experiment. However, the energies of the two high-energy LVMs of the low-spin states are resolvable and distinct from the energy of the high-spin state. Interpreting the highest energy ZPL of the triplet as the low-spin *k* site defect, the midline as the pair of high-spin centers (unresolved), and the lowest energy ZPL of the triplet as the low-spin *h* site defect gives agreement between the values of Mattausch *et al.*[6] and those of the experiment within 2 meV. By turning next to the lower-energy LVMs (M1), the same interpretation of our data gives agreement with the values of Mattausch *et al.*[6] to within 6 meV. The coexistence of these four centers was anticipated in the theoretical work.

Further confirmation of the correctness of the interpretation of our results in terms of the dicarbon antisite defect comes from the calculation of Mattausch *et al.*[6] (see Fig. 5 of Ref. 6) for a 3*C*-SiC sample with 1/3 of the C atoms replaced by ^{13}C. This calculation predicts a threefold splitting of the highest energy LVM (M2) into three component lines with energies and an intensity distribution similar to what we observed and with a value of 1.04 for the ratio of the energy of the highest energy mode to that of the lowest energy mode. The calculated LVM (M1) energies for the high-spin mode in the isotopically enriched sample (modes 3 and 4, lower panel of Fig. 5 of Mattausch *et al.*[6]) are too close to be resolved in our experiments, but the envelope of the individual peaks in their figure has a double maximum, as we observed (see Fig. 5, lower curve). The ratio of the energies of the two maxima is about 1.03, similar to what we experimentally found. However, the calculation needs to be repeated with 4*H*-SiC in order to make a reasonable comparison with our experimental results.

Accurate calculations of the excited states of optical centers are not yet achievable. However, Eberlein *et al.*[10] calculated by LDA methods that the spin tripled form of the dicarbon antisite defect of 4*H*-SiC in its neutral charge state has close-by single and double donor levels at $E_v+1.58$ eV and $E_v+1.48$ eV, respectively. These values are quite different from that calculated by Gali *et al.*[5] using a mixed Hartree–Fock correction of the Kohn–Sham level. They obtained a doubly degenerate $S=1$ state (for 3*C*-SiC) at $E_v+1.1$ eV.

C. Formation of dicarbon antisites and conditions for their observation

The experiments described here make it clear that there are two completely different ways of arriving at the observation of the 463 nm triplet. As this complex and interesting situation appear to be without precedent in previous literature, it will be explored next after a summary of the relevant results.

For 488 nm excitation, a high electron dose $\geqq 10^{19}$ e/cm^2 is required, the excitation is by up-conversion, it is approximately linearly dependent on laser power, and the emission is only weakly temperature dependent for temperatures up to about 50 K. The spectrum is strictly limited to the irradiated region, the high-spin state is relatively strongly excited for normal laser incidence, compared with 325-nm-excited emission, and the spectrum disappears from samples annealed at 950 °C. For 457.9 nm excitation, the properties are similar to those for 488 nm except that the emission is then of lower-energy photons than the laser photons.

For 325 nm excitation, at low laser power, no triplet emission could be detected. However, with an increase in laser power, the emission intensity grew with time of exposure and remained present thereafter in the exposed regions for anneals up to 800 °C. For electron doses $\geqq 10^{19}$ e/cm^2, the triplet emission was restricted to regions surrounding the irradiated area, but was not found within it. However, for 10^{18} e/cm^2, the emission came from within the irradiated area, not from outside it. The low-spin states were more strongly excited than the high-spin states for normal laser incidence. For samples that had not been annealed, the creation of the 463 nm triplet by an intense 325 nm beam was associated with the loss of intensity of those alphabet lines (*b*, *c*, and *d*) that were largely concentrated outside the irradiated area for these dose levels (but not for a dose of 10^{18} e/cm^2). However, even when the alphabet lines were

TABLE IV. Deduced correlation between the calculated and experimental results for the higher-energy LVMs in meV.

(1) exp	*k* (ls theory)	(2) exp	*k*, *h* (hs theory)	(3) exp	*h* (ls theory)
179.86	178.0	178.47	177.05	180.03	179.4

eliminated after higher annealing temperatures, an intense 325 nm beam still created a strong triplet emission in a peripheral region around the irradiated area where little, or no other, optical emission was observed.[1]

From these observations, it can be concluded that an intense 325 nm beam is able to create the 463 nm triplet in a form that is stable up to at least 800 °C. It has been calculated that the energy of formation of $(C_2)_{Si}$ is 7.8 eV in 4*H*-SiC (Ref. 6) and that adding a carbon split interstitial to a carbon antisite, to form $(C_2)_{Si}$, leads to an energy gain of 3.9 eV.[5] Preexisting carbon antisites may well be present in some of the samples that were subsequently subjected to electron irradiation. Their low energy of formation and growth under C-rich conditions favor their incorporation. These may well contribute to the mentioned variability of our results, but additional carbon antisites must be created in order to explain the high density of the defects observed. As the triplet spectrum has been observed for operating voltages well below 250 kV, the minimum required to cause Si displacement,[2] another mechanism or mechanisms rather than a direct displacement must be involved (D_1 PL is also observed at voltages well below 250 kV and is held by some to involve a nearest-neighbor antisite pair and by others to be formed by a silicon antisite defect). The creation of triplet luminescence by intense 325 nm exposure, and the associated loss of some alphabet lines, provides evidence that such a mechanism exists. Note that the spatial distribution of the alphabet lines, quenched as they are in the irradiated region for high electron doses, but extending well outside the irradiated area, is similar to that of the triplet centers created. The alphabet lines are widely accepted to result from the creation of carbon interstitials, and a recent publication[11] proposes that the $a-d$ lines arise from close-by antisite pairs. In a related publication,[12] it is argued that a supply of holes and electrons makes the formation of antisite pairs highly likely and, since the 325 nm laser involves 3.8 eV photons, a mechanism for converting an as yet unidentified carbon interstitial complex into a dicarbon antisite appears to be plausible. The fact[1] that the 463 nm triplet can be created after the elimination of the alphabet lines by high-temperature annealing indicates that other routes to their creation also exist.

A question arises as to why the triplet is not normally observed at the center of the irradiated region under 325 nm excitation. This may be related to the existence of the triplet, produced by up-conversion with 488 nm excitation, which we discuss next. It should be emphasized that the property of up-conversion is shared with several other optical centers having higher energy than the incident photons, including D_1 luminescence.[13] The continuity of the PL curve across the holographic notch filter [Fig. 1(a)] indicates that a similar excitation process exists for centers with lower energy than the incident photons (and hence is possibly responsible for the triplet specimen observed with 457.9 nm excitation). The approximately linear dependence of the triplet intensity on the increase in the 488 nm laser power indicates that two- or multiphoton processes are not important. The relative decrease in intensity of the 463 nm triplet with an increase in specimen temperature indicates the lack of phonon involvement in up-conversion. It therefore seems likely that the excitation process involves two independent centers, both absorbing energy from the incident beam with energy transfer between them. Two well-known candidate processes for energy transfer between defect centers exist. One is known as the Fŏrster–Dexter mechanism, which has been quite widely studied and is well understood.[14] The other, the defect Auger process, is less well documented.[15] Unlike quantum mechanical tunneling, the Fŏrster–Dexter process, involving resonant electromagnetic interaction between the centers, is quite long range, extending up to about 10 nm. The vibronic coupling of all the centers that is evident in this part of the spectrum would facilitate resonant transfer over a wide and continuous range of energies. Such a mechanism would only operate for a very high density of defects, which is consistent with the high electron doses that are required to see the 488-nm-excited triplet. It is evident that the existence of the optical centers responsible for the triplet alone is not sufficient because, under 488 nm (and 457.9 nm) excitation, the emission is limited to the irradiated area itself even when additional centers have been produced outside it by 325 nm exposure. At 300 keV, carbon atoms will be very efficiently displaced by the incident electron beam so that the rate of production of one displacement per centimeter path length, deduced for diamond,[16] can be used to make estimates for the defect densities created here. For a dose of 10^{20} e/cm^2, a defect density of about $10^{20}/\mathrm{cm}^3$ would be generated, which is high enough to make the Fŏrster–Dexter mechanism effective. According to this model, the triplet center would be excited to a metastable state until it receives excitation from the second center, rather like the sensitizer/activator process in phosphors. There are various forms of the defect Auger process,[15] but all require the transfer of charge. At present, it seems likely that the 463 nm centers are in neutral charge states. There is some evidence that the optical centers are isoelectronic in nature as was assumed by Gali *et al.*[5] If the relationship to the P-T lines in 6*H*-SiC is correct (see Sec. V), then their energies should scale with the band gap as observed.[3] Against this is the observed decay time which, at <10 ns, is rather short for isoelectronic centers. Auger transitions are favored under conditions of high carrier density, but these results were obtained in samples with low doping levels and the transfer did not occur under above-band-gap illumination when there would have been a high carrier density created. The balance of the evidence available seems to be against an Auger process. One other possibility is suggested by the very detailed work on the sulfur-related metastable luminescence[17] center in silicon, on which much careful work was conducted over a period of more than ten years. This center, which has been established as isoelectronic in nature, can also be excited by up-conversion. Its conversion from one form to another with below-band-gap illumination has been shown to be driven by an indirect two-step excitation process involving the transfer of an electron and a hole from unrelated deep levels.

The loss of the triplet spectrum at the center of the irradiated area, under 325 nm excitation, was accompanied by its gain there under 488 and 457.9 nm excitations. It seems, therefore, that there is a connection between these observations. The important point is to explain why 488 nm excitation succeeds in generating luminescence there while 325 nm excitation does not, yet the situation is reversed outside this

region. The simplest possible explanation would involve a single defect created by the high-dose irradiation. For example, a defect that is responsible for up-conversion before ionization by 325 nm excitation but becomes a very efficient nonradiative carrier recombination center once ionized. A somewhat similar behavior was recently reported in the case of the PL spectra from electron-irradiated cubic boron nitride.[18] It was concluded that the 325 nm excitation ionized a deep center in the irradiated area that was acting as a killer center for the excitation of PL under 488 nm excitation. These interesting problems clearly call for a more detailed investigation in the future.

The present lack of understanding about the excitation process of the triplet emission precludes an interpretation of the slightly more rapid loss of intensity from the central line of the triplet on annealing and of the marked differences of relative intensities of the low- and high-spin ZPLs under different excitation conditions. On the other hand, the survival of the central line to slightly higher temperatures in PL experiments is consistent with the theoretical evidence that the high-spin state has a slightly lower energy than the low-spin states since the calculations imply that the excited state must be near the conduction band edge.

D. Relationship to other centers created by electron irradiation

An important remaining issue is the possible relationship between the 463 nm triplet in 4*H*-SiC and the P-T lines in 6*H*-SiC. While there are many similarities, important differences also exist. Much has been made of the problem created by the reported existence of five ZPLs in 6*H*-SiC. A paper[1] associated with this deals with the other C-interstitial related centers with LVMs that were identified during the present series of experiments. One of these, having some characteristics in common with the 463 nm triplet, is a ZPL at 540.6 nm. It has similar LVM energies, annealing properties, and up-conversion. Although it can be observed with both 488 and 325 nm excitations, it is not created by an intense 325 nm beam and it lacks the nonlinear properties exhibited by the 463 nm triplet. It is apparently a single optical center. It may be that the P ZPL of 6*H*-SiC is the counterpart of this additional center, for which no really convincing atomic model exists at present. The work on the P-T centers did not include up-conversion because both excitation wavelengths used to study these centers involved photons of higher energy. However, the spatial distribution of the P-T centers was similar at both 488 and 325 nm excitation wavelengths and no nonlinear behavior on the time dependence of the spectra was found under 325 nm excitation. On the other hand, there may, in fact, be an additional ZPL in 6*H*-SiC related to the P-T lines that has not yet been reported. The quality of the material used for the reported 6*H* experiments was much inferior to the 4*H* material used in these experiments, and there were certainly other ZPLs present in the relevant spectral range.

V. SUMMARY AND CONCLUSIONS

The experiments performed show that, for large enough electron doses $\geqq 10^{19}$ e/cm^2 and energies greater than 200 keV, centers are formed at room temperature that are associated with a 463 nm triplet of ZPLs. These centers are stable up to high temperatures and have properties that clearly identify them as dicarbon antisite defects. There is excellent agreement with the results of recent LDA calculations. In fact, there are four distinct ZPLs for these defects, two (T1 and T4) in an $S=0$ spin state and two (T2 and T3) in an $S=1$ spin state, with the two lines corresponding to defects on the pseudocubic (k) and two for the pseudohexagonal (h) sites. The two high-spin defects have ZPLs and LVMs that are too close for us to be able to resolve them in our experiments.

The excitation properties of these centers are quite remarkable and strongly dependent on the excitation wavelength. For 457.9 or 488 nm excitation, the triplet is only found within the irradiated region itself. For 488 nm excitation, the triplet occurs by up-conversion, which is linearly dependent on the laser power: it is no longer detected after 900 °C anneals. A Förster–Dexter mechanism is proposed as an explanation for the up-conversion process with a nonradiative deep center transferring energy to the triplet, a process that terminates when the deep center anneals out. For 325 nm excitation, at low power, the triplet is not observed, but it increases in a time-dependent, superlinear fashion on exposure to higher laser powers and then remains enhanced on returning to the original laser power. The enhanced emission is principally located outside the irradiated region and has a triplet with very different intensity distribution, with the middle line greatly reduced in intensity. The local enhancement remains after high-temperature anneals up to 800 °C and can still occur up to 1300 °C but vanishes at higher temperatures. It is concluded that the 325 nm beam causes changes in atomic arrangement, which create the dicarbon antisite center. This work demonstrates that dicarbon antisite defects are created after room temperature electron irradiation of 4*H*-SiC at electron energies below that required to displace silicon atoms.

ACKNOWLEDGMENTS

The authors wish to thank the Engineering and Physical Sciences Research Council (UK) for support of this work, G. Wagner (Institute for Crystal Growth, Berlin) for supply of material, F. Phillipp (Stuttgart) and U. Dahmen (Berkeley) for access to high voltage TEMs, and N. G. Wright for high-temperature annealing of samples. We are also grateful to A. Gali and A. Mattausch for a discussion of their calculations, and J. Hayes for performing the time-dependence measurements. Technical assistance in sublimation growth of ^{13}C enriched samples was kindly provided by Y.-S. Jang and S. A. Sakwe (Erlangen).

[1] J. W. Steeds and W. Sullivan, Phys. Rev. B **77**, 195204 (2008).
[2] J. W. Steeds, F. Carosella, G. A. Evans, M. M. Ismail, L. R. Danks, and W. Voegeli, Mater. Sci. Forum **353-356**, 381 (2001).
[3] J. W. Steeds, G. A. Evans, L. R. Danks, S. Furkert, W. Voegeli, M. M. Ismail, and F. Carosella, Diamond Relat. Mater. **11**, 1923 (2002).
[4] G. A. Evans, J. W. Steeds, L. Ley, M. Hundhausen, N. Schulze, and G. Pensl, Phys. Rev. B **66**, 035204 (2002).
[5] A. Gali, P. Déak, P. Ordejón, N. T. Son, E. Janzén, and W. J. Choyke, Phys. Rev. B **68**, 125201 (2003).
[6] A. Mattausch, M. Bockstedte, and O. Pankratov, Phys. Rev. B **70**, 235211 (2004).
[7] Y.-S. Jang, S. A. Sakwe, P. J. Wellmann, S. Juillaguet, H. Peyre, J. Calmassel, and J. W. Steeds, Mater. Sci. Forum **556-557**, 13 (2007).
[8] T. Egilsson, A. Henry, I. G. Ivanov, J. L. Lindström, and E. Janzén, Phys. Rev. B **59**, 8008 (1999).
[9] J. W. Steeds, Mater. Sci. Forum **556-557**, 313 (2007).
[10] T. A. G. Eberlein, R. Jones, P. R. Briddon, and S. Öberg, *Semiconducting Defect Engineering – Materials, Synthetic Structures and Devices*, MRS Symposia Proceedings No. 864 (Materials Research Society, Pittsburgh, 2005), p. E1.2.1.
[11] T. A. G. Eberlein, R. Jones, S. Öberg, and P. R. Briddon, Phys. Rev. B **74**, 144106 (2006).
[12] T. A. G. Eberlein, C. J. Fall, R. Jones, P. R. Briddon, and S. Öberg, Phys. Rev. B **65**, 184108 (2002).
[13] J. W. Steeds, S. A. Furkert, W. Sullivan, and G. Wagner, Mater. Sci. Forum **527-529**, 433 (2005).
[14] See, M. D. Crossfield, G. Davies, A. T. Collins, and E. C. Lightowlers, J. Phys. C **7**, 1909 (1974); D. L. Dexter, J. Chem. Phys. **21**, 836 (1953).
[15] See, for example, A. Hangleiter, Phys. Rev. B **37**, 2594 (1988).
[16] G. Davies, Physica B (Amsterdam) **273-274**, 15 (1999).
[17] P. W. Mason, H. J. Sun, B. Ittermann, S. S. Ostapenko, G. D. Watkins, L. Jeyanathan, M. Singh, G. Davies, and E. C. Lightowlers, Phys. Rev. B **58**, 7007 (1998).
[18] E. M. Shishonok and J. W. Steeds, Diamond Relat. Mater. **11**, 1774 (2002).